Cosmic rays acceleration at ultrarelativistic subshocks

Janusz Bednarz

Uniwersytet Warmińsko-Mazurski, Wydział Matematyki i Informatyki, ul. Żołnierska 14, 10-561 Olsztyn, Poland
bednarz@matman.uwm.edu.pl

Abstract

We present the model of cosmic rays acceleration at ultrarelativistic subshocks and confront it with the observations of gamma-ray bursts (GRBs) and blazars. We investigate cosmic rays acceleration in shocks with Lorentz factors (γ) in the range 3 - 40. We show that fluctuations of the magnetic field downstream of the shock do not play an important role in the acceleration process. Results of numerical simulations for shocks with considered Lorentz factors and perpendicular magnetic field inclinations are presented. We fit the derived particle energy spectral index (σ) dependence on fluctuations of the magnetic field upstream and γ with a function.

Key words: acceleration of particles – shock waves – gamma rays: theory

1. Introduction

The acceleration mechanism which operate at ultrarelativistic shock fronts was discovered by Bednarz & Ostrowski (1998). The mechanism is different from the diffusive particle acceleration which is assumed to be suppressed at superluminal shock fronts (Bell 1978; Drury 1983). The effect of the magnetic field direction is important for ultrarelativistic shocks because all of them are superluminal. Medvedev & Loeb (1999) have shown that the relativistic two-stream instability naturally generate strong magnetic fields which are parallel to the shock front. Therefore ultrarelativistic shocks have to be superluminal even if one could imagine an external magnetic field with the angle between the upstream field and the shock normal smaller than $\sim 1/\gamma$. Ultrarelativistic shocks without any mean magnetic fields cannot be considered as real physical phenomena by the same reason.

It have appeared a few papers about a particle acceleration at ultrarelativistic shocks without mean magnetic fields (Kirk et al. 2000; Achterberg et al. 2001; Vietri 2003; Lemoine & Pelletier 2003) or with subluminal shock geometry (Ellison & Double 2002 - parallel shocks). Their acceleration is similar to the diffusive shock acceleration but it includes anisotropies in the angular distribution upstream of the shock. However, particles in this acceleration are able to return to the shock from downstream to upstream due to large magnetic field fluctuations downstream of the shock or due to subluminal shock geometry as in non-relativistic and mildly relativistic regime. Thus, they have failed to understand the actual ultrarelativistic shock acceleration mechanism because the returning is due to small fluctuations of the magnetic field upstream of the shock (the needed fluctuations decrease when the Lorentz factor of the shock increases) and relativistic effects providing a small change of the particle trajectory in the mean field upstream of the shock to be large as measured downstream. To date, the only numerical calcula-

tions performed by Bednarz & Ostrowski (1998), Bednarz (2000) and in this paper consider the problem of particle acceleration in ultrarelativistic shocks.

It is known for a long time that relativistic shocks occur in regions of efficient acceleration of leptons. The acceleration to non-thermal distributions is observed at hot spots of extragalactic radio sources, in blazars, GRBs and pulsar wind nebulae. In order to account for the presence of these high energy leptons, some authors have tried to find the acceleration mechanism. Begelman & Kirk (1990) proposed shock-drift acceleration at relativistic shocks to operate at hot spots of extragalactic radio sources. In the mechanism, particles are accelerated in a single shock crossing by drifting parallel (or anti-parallel) to the electric field. Afterwards, Hoshino et al. (1992) described a process of shock acceleration of positrons to non-thermal distributions devoted to account for the synchrotron radiation observed in the Crab Nebula and hot spots. In the model, the gyrating reflected protons downstream of the shock dissipate their energy in the form of collectively emitted, left-handed magnetosonic waves which are resonantly absorbed by the positrons immediately behind the ion reflection region. The dynamics of the Weibel instability has recently been simulated by several research groups using 3D plasma kinetic code. These simulations confirm both the generation of the magnetic field and the particle acceleration downstream of the shock. The particle energising in Silva et al. (2003) simulations (electron-positron plasma) is due to pitch angle scattering in the produced magnetic field after saturation. The energy stored in the magnetic field is transfered back to the plasma particles. Simulations of Frederiksen et al. (2003) have yielded the energy transfer from protons to leptons similar to Hoshino et al. (1992). In their description, the scattered protons create a fluctuating electric field which tends to equilibrate the energy between protons and electrons. Nishikawa et al. (2003) results suggest that electrons and ions are accelerated in the direction transverse to the shock normal

only.

All the described mechanisms suffer from small energies the particles are able to acquire. The shock-drift acceleration allow for the energy increase of about ten times. Leptons can receive the energy from protons which is about ten times ($\sim \gamma$ times in Frederiksen et al. 2003 does not necessarily depend on γ) above the thermal energy downstream of the shock. Silva et al. (2003) simulations have led to the generation of high-energy tails in the distribution function, with energies few times above the thermal energy downstream of the shock. In our model presented below, we apply some of these mechanisms to production of seed particles.

2. The model of cosmic rays acceleration at ultrarelativistic subshocks

In the model, we assume an extremely relativistic outflow of electrons and positrons and probably protons and nuclei which originates from a central engine. The outflow consists of few portions of uniform plasma. These portions have different Lorentz factors and relative Lorentz factors between some of them reach value from several up to tens. Temperatures of these portions are similar to each other.

In the first phase of the acceleration process, leptons and baryonic matter are preaccelerating either in the shock generated by the first slab of the outflow hitting the material around the central object or in the shock created by two colliding slabs. Depending on γ, seed particles are producing in the forward and reverse shock or in the forward shock only.

After the collision the temperature of the resulting plasma is higher than temperatures of the two slabs before the collision. We expect that the external magnetic field influences to the dynamics of the Weibel instability in such a way that the magnetic field produced by the instability is oriented in the form of a toroidal magnetic field. It has been suggested that hoop stresses associated with toroidal fields wrapped around the extragalactic jet will pinch the outflowing plasma and exert in this way a collimating force on the jet. Following that example, we expect that the heating plasma will only expand in the direction parallel to its velocity. In result, the collision yields a very long and hot jet filled with seed particles and toroidal magnetic field.

We distinguish between dense enough and very thin material of electrons, protons and probably nuclei surrounding the site of the central engine. If the material is very thin, then protons or nuclei must be present in the outflow to allow for leptons acceleration thanks to the energy transfer from baryons (mechanisms: Hoshino et al. 1992, Frederiksen et al. 2003). If the preacceleration takes place in two colliding slabs of electron-positron plasma, then Silva et al. (2003) mechanism is being the only one at work.

In the second phase, a following slab of plasma is catching up with the plasma filled with non-thermal relativistic particles. These particles are rapidly accelerating in the ultrarelativistic shock acceleration mechanism if the Lorentz factor of the formed shock is large enough. Afterwards, they flow downstream of the shock and continually radiate synchrotron radiation. The maximum energy the particles are able to reach is determined by the size of the shock or by the value of the magnetic field fluctuations upstream of the shock and γ or by the acceleration time (it is very short, see Bednarz 2000) and the plasma rest frame magnetic and radiative energy density. However, only a few per cent of seed particles are involved in the process by reason of small efficiency of cosmic ray reflections (Bednarz & Ostrowski 1999).

The presented scenario is capable of explaining many features of GRBs and some features of blazars as well. The occurrence of the two phases of the acceleration is one of them. Ghisellini et al. (2002) have derived from spectral properties of blazars that a phase of pre-heating and a phase of rapid acceleration leading to a non-thermal distribution occur by turns in these objects. In GRBs, the first phase is observed in the form of the precursor which was detected in a few per cent of GRBs only (Koshut et al. 1995). The rare occurrence of precursors is best explained by small energy of seed particles that strongly depends on γ.

In the main phase of the acceleration, the shock slows down in consequence of collecting slower material from upstream. In the phase we distinguish two sub-phases. First, both the reverse and the forward shocks are present and the speed of the forward shock is constant. Next, the reverse shock disappears on the edge of the back slab and the forward shock slows down. The long and hot slab of plasma filled with seed particles and toroidal magnetic field is much longer than the slab of plasma originating from the central engine. In consequence, the reverse shock disappears in much shorter time than the forward shock crosses the plasma and we can neglect the first sub-phase.

Further on, we consider that the maximum energy of particles in GRBs is determined by the value of magnetic field fluctuations upstream of the shock and γ (we neglect the fraction of particles with large spectral indices) and consider constant spectrum of magnetic field fluctuations upstream of the shock. As will be shown further, the spectral index of accelerating particles with momenta larger than a threshold momentum p_t increases and simultaneously, it remains for the others approximately constant as long as γ decreases. Moreover, p_t decreases when the shock slows down. The rising phase of the GRB pulse is attributed to the energising of seed particles but the peak in the light curve is shifted in different energy channels. The GRB lag (Kocevski & Liang 2003) arises from decreasing p_t. When first particles reach $p_t(t=0)$ with $\sigma \approx \sigma_l$ (one should choose σ slightly larger than σ_l - the limiting spectral index), the following ones reach $p_t(t=0)$ with $\sigma > \sigma_l$ because $p_t(t>0) < p_t(t=0)$. In result, the excess of particles at p_t moves towards smaller momenta producing the observed lag. Similarly, the detected spectral evolution of main pulses (Crider et al. 1997; Ghirlanda et al. 2002) arises due to increasing the energy of particles with constant $\sigma \approx \sigma_l$ in the rising phase and increasing σ of particles with momenta larger than p_t in the decaying

phase.

Many shapes of main pulses resemble a FRED (fast rise, exponential decay). The rising phase of pulses produced by shocks with larger initial γ must yield steeper light curves than the phase produced by slower shocks. The main reason of this is the reduction in the compression of the magnetic field which, in turn, causes the increase of the acceleration time (equal to $\sim r_g/c$ - Bednarz 2000, r_g - is the particle gyroradius and c - the speed of light). The decaying phase is long because particles are still accelerating but it can be fast if the shock producing the main pulse comes to the region without seed particles before particles reach p_t. The reverse shock could supply with seed particles less efficiently than the forward shock can and the light curve will exhibit two peaks when a following shock ploughs into such plasma. One could also imagine a break in the field of seed particles if two shocks generate it independently.

We propose that short variability timescale pulses, which overlap on main pulses, arise from interaction between the magnetic field generated by the shock and a strong external magnetic field or the toroidal field of the hot forward plasma. That interaction can produce fast changes in direction of the shock velocity (similar to gyration) and, by turns, the sub-pulses because the detected flux strongly depends on the angle between the shock normal and the direction of observation.

Most of the particle spectral indices in blazars (Ghisellini et al. 2002) and in GRBs are in good agreement with the value of 2.18 and larger derived for ultrarelativistic shocks in this paper. Suggesting smaller value of σ (Panaitescu & Kumar 2002) is naturally explained by a jet model with continuous energy injection and σ above 2.18 (Björnsson et al. 2002). The continuous energy injection is in agreement with the presented model. In some of the GRBs events, the last slab (or a group) of plasma can be the slowest one. First, the distance between the forward and the backward plasma is increasing and the forward plasma is collecting interstellar matter and slowing down. Next, the distance is decreasing and finally, the backward plasma hits the forward one and forms a shock. We expect that, in many cases, γ of the shock is large enough to allow for the acceleration across the main mechanism. The forward material is in the form of long, thin jet with the Lorentz factor considerably smaller than at the GRB stage. The external magnetic field is much weaker than the field near the central engine. All the reasons influence that the detecting radiation is below X-ray range and is lasting for long time. The colliding jets are responsible for breaks in the afterglow light curves.

There is an open question if relativistic shocks can produce seed protons and nuclei. The simulations of Nishikawa et al. (2003) suggest that they could. Heavy particles in a cold plasma upstream of the shock are seeing a shock generated by leptons as a discontinuity but they are not ultrarelativistic there. We suggest that seed baryons could be produced in a mechanism similar to shock-drift acceleration in these shocks if leptons taking away the energy from baryons downstream of the shock remain the fraction of total baryons which end up with super-thermal energies. In this picture, the ultrarelativistic shock acceleration mechanism could produce a major part of the cosmic rays.

3. Simulations

In simulations we follow the procedure used by Bednarz & Ostrowski (1996) with a hybrid approach used by Bednarz & Ostrowski (1998). Monoenergetic seed particles are injected at the shock with the same initial weight factor. Each particle trajectory is followed using numerical computations until the particle escapes through the free escape boundary placed far downstream from the shock or it reaches the energy larger than the assumed upper limit. These particles are replaced with the ones arising from splitting the remaining high-weight particles in a way to preserve their phase space coordinates, but ascribing only a half or a smaller respective part of the original particle weight to each of the resulting particles. All computations are performed in the respective upstream or downstream plasma rest frame. Each time the particle crosses the shock its momentum is Lorentz transformed to the respective plasma rest frame and, in the shock normal rest frame, the respective contribution is added to the given momentum bin in the particle spectrum. We derive the particle trajectories in the mean magnetic field and a fluctuating component. The perturbed magnetic field represents the traditional picture based on the concept of magnetic scattering centres. It is simulated by small amplitude particle momentum scattering within a cone with angular opening $\Delta\Omega$ less than the particle anisotropy $\sim 1/\gamma$. The particle momentum scattering distribution is uniform within the cone. The time (measured in r_g/c) between scatterings is uniformly distributed from $0.5t_{d,u}$ to $1.5t_{d,u}$ (t_d and t_u are mean times between scatterings downstream and upstream respectively). After crossing the shock, the remaining time the particle should follow in the mean field before the next scattering is multiplied or divided by t_d/t_u. Particle energy is preserved at each scattering in the plasma rest frame. For the considered continuous injection after initial time, the energy cut-off of the formed spectrum shifts toward higher energies with time. The resulting spectra allow one to fit spectral indices and derive acceleration time. The downstream magnetic field, its inclination to the shock normal and shock speed are derived for the relativistic shock with the compression $R_h = 3U_1^2$ (U_1 is the shock speed) for the hot plasma. In the simulations presented in Fig. 2, we applied compression R_c obtained with the formula of Heavens & Drury (1988) for a cold proton-electron plasma.

In order to estimate the correctness of R_h for slow shocks, we followed the computations of Heavens & Drury (1988). The bottom panel of Fig. 1 shows the difference between R (the real compression) and R_h as a function of γ for some cases of the upstream fluid (T_p, T_e - the upstream temperature of proton-electron, electron-positron plasma in units of $5.4 \cdot 10^{12}K$, $5.9 \cdot 10^9K$ respectively). The top panel shows the relation between γ and the down-
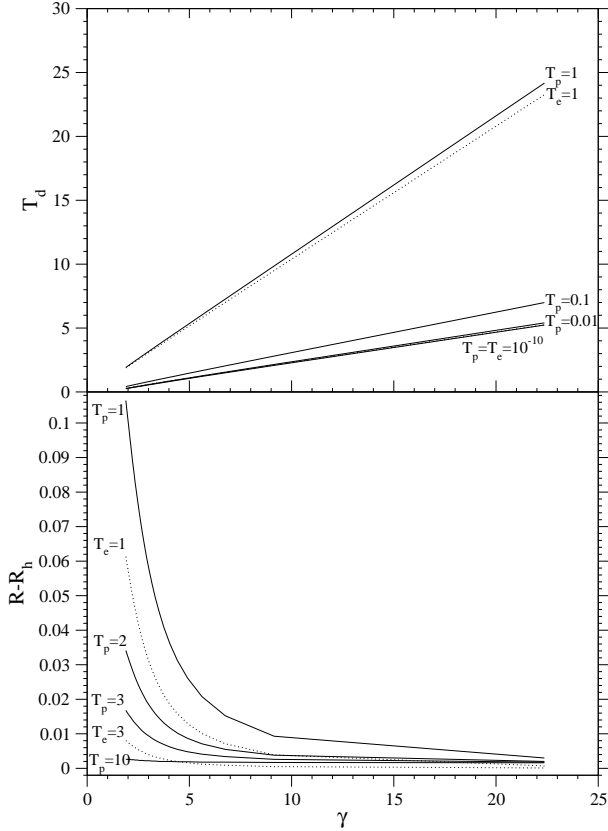
Fig. 1. The downstream temperature and the difference between the compression and the compression of the hot plasma limit as a function of the shock Lorentz factor. The curves correspond to different upstream temperatures and are marked with T_p (solid curves) or T_e (dotted curves). In the upper panel, $T_p = T_e = 10^{-10}$ is close to $T_p = 0.01$.

stream temperature (T_d - in the same unit as appropriate $T_{p,e}$). We can draw a conclusion that γ of the shock hitting a cold plasma must be larger than 6 during the preacceleration so that R_h might be adequate for shocks with $\gamma < 5$ in the main phase.

4. Some features of the acceleration mechanism

We have performed simulations in the absence of magnetic field fluctuations upstream and for a few cases of the fluctuations downstream measured by a parameter $\lambda = log(\frac{\kappa_\perp}{\kappa_\parallel})$, where $\kappa_\perp$ and $\kappa_\parallel$ are perpendicular and parallel diffusion coefficients respectively. We have chosen a few values of γ and the upstream magnetic field inclination with respect to the shock normal $\psi = 10°, 30°, 90°$. We exhibit the outcome of the simulations in Fig. 2 . The large value of σ for $\psi = 10°$ and $\gamma = 3$ arises due to escaping a large fraction of particles far upstream from the shock. The σ dependence on ψ or γ is present for large value of σ only. We have obtained $\sigma = 2.5; 3.5; 5$ for $\lambda = 0; -0.16; -0.67$ respectively.

As was shown above, medium-value magnetic field fluctuations downstream can be neglected in the acceleration. We suspect that they are really small if we take

into account very high linear polarization reported in RHESSI observations of GRB021206 (Coburn & Boggs 2003). Moreover, the particles do not interact resonantly with magnetic field perturbations upstream since the time between shock crossings downstream-upstream and upstream-downstream is a small part of r_g/c. Therefore, our scattering model is the best because it reproduces the non-resonant interactions excellently and independently of magnetic field fluctuations spectra. The model follows the relation $\frac{\kappa_\perp}{\kappa_\parallel} = \frac{1}{1+const(\omega\tau)^2}$, τ is the mean time when the particle momentum (p) direction shifts at an angle smaller than 20° because of scatterings and ω is the gyration frequency. Let us introduce the ordinary assumption that each fluctuation shifts the direction at a small angle $\sim 1/p$. As a result, $\tau \sim p^2$ and subsequently, $\frac{\kappa_\perp}{\kappa_\parallel} = \frac{1}{1+Qp^2}$ (Q results from fluctuations spectra). For large p we get $\lambda = -2log_{10}(Qp)$. Eq. (1) yields that λ upstream increases (p decreases) with decreasing γ and constant σ. That is the reason for the lag in GRBs light curves.

The angular distribution of particles at the shock in the downstream plasma rest frame presented by Bednarz & Ostrowski (1998) peaks at $\mu = -U_2$, U_2 is the shock speed in the downstream rest frame and μ is the cosines of the angle between the shock normal and the particle momentum. The distribution presented by other authors peaks at $\mu \simeq 0$ but they did not follow full 3D simulations (or calculations) with the mean field and we cannot compare the results because it is difficult for us to mimic the reduced situations. We expect the peak at $-U_2$ arises from keeping a fraction of particles close to the shock. The particles contribute to the distribution considerably because their velocities perpendicular to the shock plane approach the shock speed. They can oscillate between upstream and downstream especially, if scatterings upstream are close to the shock plane. In Fig. 3, we present the simulations for $\gamma = 27$, $\psi = 90°$, different $t_{d,u}$ (the diffusion is the same because $\Delta\Omega^2/t_{d,e} = const$) and $\lambda = 0$. The distribution function narrows with decreasing $t_{d,u}$ but σ does not change.

The explanation of the shift in the distribution function presented by Ostrowski & Bednarz (2002) is false[1]. It is obvious that the absolute value of the inverse of the relative particle velocity with respect to the shock is the particle weight. One obtains unlike distribution if one applies the velocity in the plasma rest frame.

We obtained the limiting spectral index for $\lambda = 0$ upstream and downstream, $\psi = 90°$ and γ from 60 to 120 (33 points). It is equal to $\sigma_{lm}(\gamma > 60) = 2.23 \pm 0.03$.

5. The relation between σ, γ and λ

In the simulations below, we have applied $t_d = 0.1$ and $\Delta\Omega = 10^{-6}$ downstream ($e^\lambda = 0$, homogeneous magnetic field) and $\psi = 90°$. First, we have found the limiting spectral index for large γ (γ from 60 to 100 - 58 points, $\lambda = 0$ upstream): $\sigma_{l0}(\gamma > 60) = 2.18 \pm 0.03$. Next, for the same

---

[1] That is not mine. M. Ostrowski did not consult with me the context of the paper.
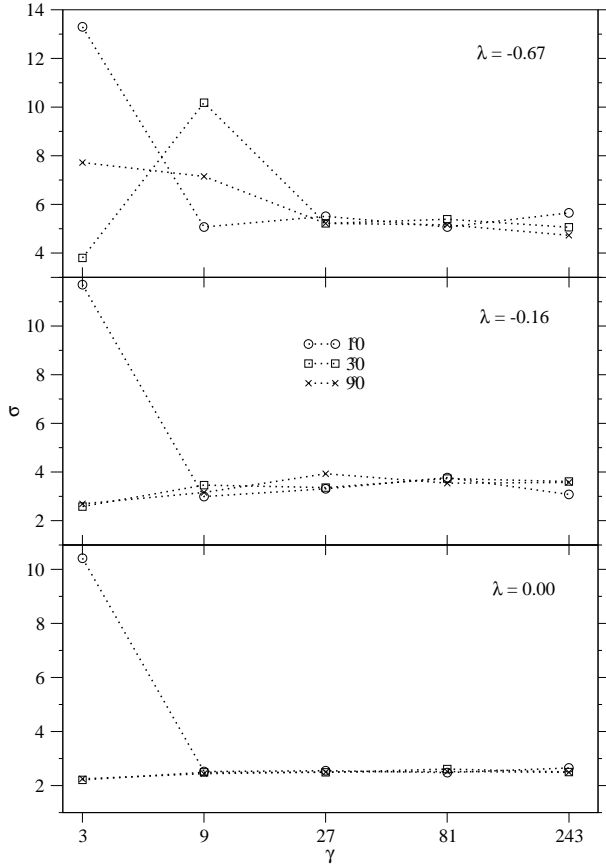
Fig. 2. Simulated spectral indices as a function of the shock Lorentz factor. Three values of the magnetic field inclination upstream of the shock are applied ($\psi = 10°, 30°, 90°$). Magnetic field fluctuations upstream are not present. Results for given downstream magnetic field perturbations λ are presented separately.
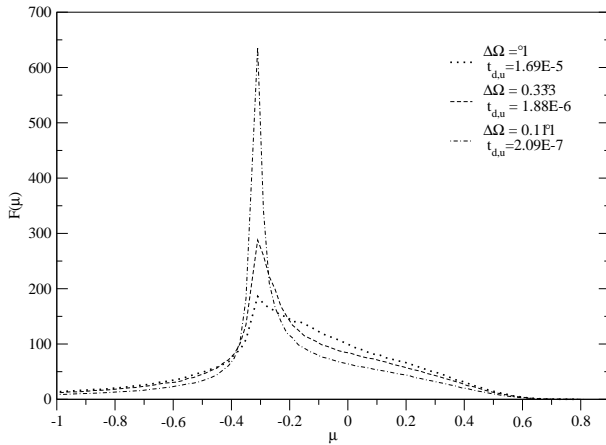

Fig. 3. Simulated particle angular distributions at the shock, as measured in the downstream plasma rest frame, for $\gamma = 27$, $\psi = 90°$ and $\lambda = 0$ (downstream and upstream). The distribution function narrows when $t_{d,u}$ decreases but σ is constant.
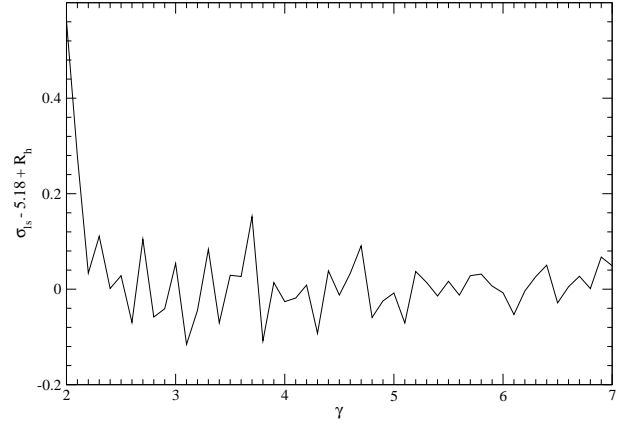

Fig. 4. The difference between the limiting spectral index obtained from simulations (σ_{ls}) and σ_l.

conditions ($\psi = 90°$ and $e^\lambda = 0$ downstream), our simulations have covered two γ ranges: 1) from 2 to 7 every 0.1; 2) from 2 to 40 every 1 and λ upstream from 0 to -4.3. Then, we have been able to obtain σ_l for $\gamma > 3$: $\sigma_l = 5.18 - R_h$ (see Fig. 4). We have continued analysis of the data. Let us introduce two parameters $r_m = R_h/3$ and $r_d = R_h - 2$. We have fitted $\sigma/\sigma_l - r_m^{3.2}$ as a function of $\lambda_p = 3.36 - 1.94 log_{10}(\gamma) - 0.3 r_d - \lambda/r_d$ for $\sigma < 7$, $\lambda_p > 0.55$ and $3 \le \gamma \le 40$:

$$\frac{\sigma}{\sigma_l} - r_m^{3.2} = K(\lambda_p^5 + 13.1\lambda_p)(1 - \frac{0.147}{\lambda_p}),$$
$$K = 4.6 \cdot 10^{-3} \pm \frac{2 \cdot 10^{-3}}{\lambda_p}. \tag{1}$$

The fitting is correct if $\lambda_p > 0$ but the error is too large and there are systematic effects if $\sigma \to \sigma_l$. We have replaced (1) with the linear function from $\sigma \approx 1.03\sigma_e$ (σ_e is the limiting σ derived from (1)) to σ_l to improve eq. (1). We have fixed the intersection of the two curves at $\lambda_{pc} = \lambda_p(\sigma \approx 1.03\sigma_e)$:

$$\lambda_{pc} = 2.86 - 0.265\gamma + 0.015\gamma^2 - 4.02 \cdot 10^{-4}\gamma^3 + $$
$$+3.88 \cdot 10^{-6}\gamma^4. \tag{2}$$

The linear function is

$$\sigma = \sigma_l(a\lambda + 1) \pm \Delta\sigma, \quad a = ((\frac{\sigma}{\sigma_l})_c - 1)/\lambda_c, \tag{3}$$

where the select error $\Delta\sigma = \sigma_l((\frac{\sigma}{\sigma_l})_c - r_m^{3.2})/(2.3\lambda_{pc})$ depends on γ only at the intersection $(\frac{\sigma}{\sigma_l})_c = 4.6 \cdot 10^{-3}(\lambda_{pc}^5 + 13.1\lambda_{pc})(1 - \frac{0.147}{\lambda_{pc}}) + r_m^{3.2}$, $\lambda_c = r_d(3.36 - 1.94 log_{10}(\gamma) - 0.3 r_d - \lambda_{pc})$ and below. An example of a curve derived from (1), (2) and (3) for $\gamma = 32$ is presented in Fig. 5 and a few curves for different γ are shown in Fig. 6. The relation between σ, γ and λ is necessary to model GRBs light curves.

Acknowledgements

References

Achterberg A., Gallant Y. A., Kirk J. G., Guthmann A. W., 2001, MNRAS, 328, 393
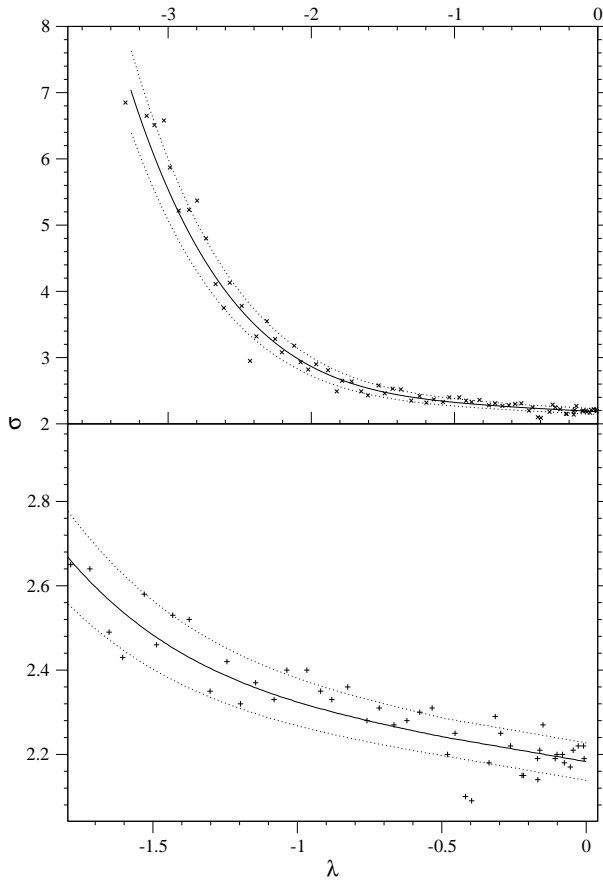
Fig. 5. The spectral index of the energy distribution function at the shock, for particles accelerated in the shock with $\gamma = 32$ propagating into hot plasma, as a function of magnetic field fluctuations upstream ($e^\lambda = 0$ downstream and $\psi = 90°$). The solid line is composed of two curves (equations (1) and (3)) with the intersection at (2). Dotted lines define the standard error and crosses represent results of simulations.
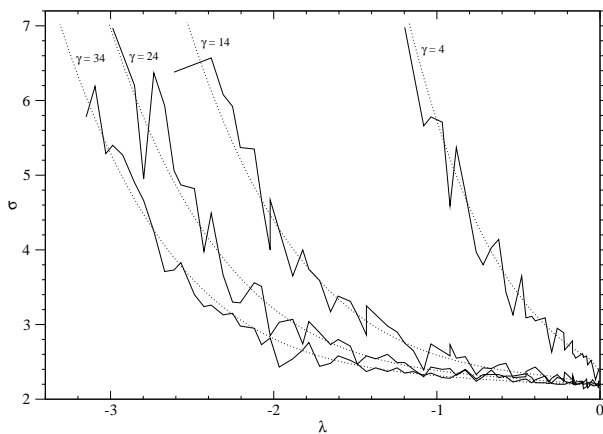

Fig. 6. The spectral index of the energy distribution function at the shock, for particles accelerated in the shock with $\gamma = 4; 14; 24; 34$ propagating into hot plasma, as a function of magnetic field fluctuations upstream ($e^\lambda = 0$ downstream and $\psi = 90°$). The numerical results are joined by the solid lines. The dotted lines represent the fit.

Bednarz J., 2000, MNRAS, 315, L37

Bednarz J., Ostrowski M., 1996, MNRAS, 283, 447

Bednarz J., Ostrowski M., 1998, Phys. Rev. Lett., 80, 3911

Bednarz J., Ostrowski M., 1999, MNRAS, 310, L11

Begelman M. C., Kirk J. G., 1990, ApJ, 353, 66

Bell A. R., 1978, MNRAS, 182, 147

Björnsson G., Hjorth J., Pedersen K., Fynbo J. U., 2002, ApJ, 579, L59

Coburn W., Boggs S. E., 2003, Nature, 423, 415

Crider A. et al., 1997, ApJ, 479, L39

Drury L. O'C., 1983, Rept. Progr. Phys., 46, 973

Ellison D. C., Double G. P., 2002, Astropart. Phys., 18, 213

Frederiksen J. T., Hededal C. B., Haugbølle T., Nordlund Å., 2003, astro-ph/0303360

Ghirlanda G., Celotti A., Ghisellini G., 2002, A&A, 393, 409

Ghisellini G., Celotti A., Costamante L., 2002, A&A, 386, 833

Heavens A., Drury L'O. C., 1988, MNRAS, 235, 997

Hoshino M., Arons J., Gallant Y. A., Langdon A. B., 1992, ApJ, 390, 454

Kirk J. G., Guthmann A. W., Gallant Y. A., Achterberg A., 2000, ApJ, 542, 235

Kocevski D., Liang E., 2003, ApJ, 594, 385

Koshut T. M., Kouveliotou C., Paciesas W. S., van Paradijs J., Pendleton G. N., Briggs M. S., Fishman G. J., Meegan C. A., 1995, ApJ, 452, 145

Lemoine M., Pelletier G., 2003, ApJ, 589, L73

Medvedev M. V., Loeb A., 1999, ApJ, 526, 697

Nishikawa K.-I., Hardee P., Richardson G., Preece R., Sol H., Fishman G. J., 2003, ApJ, 595, 555

Ostrowski M., Bednarz J., 2002, A&A, 394, 1141

Panaitescu A., Kumar P., 2002, ApJ, 571, 779

Silva L. O., Fonseca R. A., Tonge J. W., Dawson J. M., Mori W. B., Medvedev M. V., 2003, ApJ, 596, L121

Vietri M., 2003, ApJ, 591, 954